Multi-Identification and Motion Control of a Two-Axis Pan-Tilt Platform

IOP Conf. Series: Journal of Physics: Conf. Series **1267** (2019) 012086 doi:10.1088/1742-6596/1267/1/012086

Multi-Identification and Motion Control of a Two-Axis Pan-Tilt Platform

Yihui Fan[1], Xingyan Zheng[1], Bin Ye[1*], Yuzhe Yang[1] and Da Zhao[2]

[1]School of Information and Control Engineering, China University of Mining and Technology
[2]School of Mechatronic Engineering, China University of Mining and Technology

[*]Corresponding e-mail: yebin@cumt.edu.cn

Abstract. The two-axis pan-tilt platform (PTP) has been widely used in industrial control systems. The control performance of the PTP is sharply affected by the load variations, which are more significant on the pitch axis. Moreover, the PTP control system is sensitive to sensor noise and the friction moment. To achieve rapid and precise control, we build a pan-tilt platform model using the method of multiple system identification and design a speed controller and position controller on both the yaw and the pitch axes. The proposed method avoids the need to measure a large number of mechanical and electrical parameters. The experimental result shows that the proposed control system has small overshoot, fast response and suitable robustness. Relative to a controller designed and adjusted by experience, the designed system increases the bandwidth by approximately 50% on the yaw axis, and the settling time is decreased.

1. Introduction

The pan-tilt platform (PTP) is well suited for a wide range of applications in real life, including surveillance, border patrol, and entertainment [1]. In addition, it is widely used in unmanned aerial systems for aerial photography [2] and target tracking [3]. A PTP system is typically driven by motors and is thus influenced by load variations and gravity torques, among other perturbations [4]. The need for a rapid and precise PTP control system is widespread. Thus, developing an accurate PTP model is vital in the design of control systems.

Existing PTP models can be divided into two types: linear models and nonlinear models. In the linear models, the centrifugal, Coulomb friction and Coriolis forces are ignored; however, they are incorporated in the nonlinear model [5]. Mechanism modeling and system identification are the two basic methods to build up a model [6]. Currently, PTP design is based primarily on mechanism modeling, and system identification methods are barely used. In the mechanism modeling of the PTP system, it is typically necessary to obtain the back electromotive force constant, torque constant of the motor, and selected physical and electrical parameters such as the moment of inertia of the PTP, which increases the challenge of developing the model. Load changes also affect the model [7]. In addition, the model accuracy may rely on the accuracy of the parameter measurement. Some parameters are hard to obtain; thus, a large deviation potentially exists between the obtained model and real model [8,9]. In [10], a biomimetic control strategy of an on-board pan-tilt-zoom camera is presented. This system can compensate the deflection caused by the flight platform and thus enhance the system performance. In [11], the active disturbance rejection control technique is applied to the tracking

control of a pan-tilt camera to improve the performance of the pan-tilt camera platform. An implementation of two fuzzy logic controllers working in parallel for a pan-tilt camera platform on an unmanned aerial vehicle is presented in [12], and the controllers have shown favorable performances in real flights for static objects. In [13], the harmonic drive model of the pan-tilt platform is put forward, which consists of a linear spring and a load inertia to represent the compliance between load side angles and the motor, this approach can better incorporate the impact of friction on the system, thus improving the accuracy of the system. A control method based on self-adaptive PID, used in a uniaxial turntable control system, is presented in [14]. The controller can solve the nonlinear and time-varying band problems of turntable system.

With the number of controllers increasing, the inconsistency between the obtained PTP model and the real model is expected to accumulate [14]. In addition, after each new controller is added, this also means control links increase, the disturbance factor is introduced due to the sensor of the parameter measurement, which is not conducive to continuing to design the controller.

The PTP considered here can realize 360º rotation around the yaw axis. Consequently, the motion interval is relatively large, and the stability requirement for the model is higher. In this paper, we treat the PTP on the pitch and the yaw axis as two independent systems, modeling them separately and designing different controllers for them. In this paper, we propose to use a multi-identification approach to develop the model instead of using mechanism modeling. By considering the PTP on each axis, we first identify its model and then establish a speed controller based on the model. The system with the speed controller should be re-identified, and the position controller is designed according to the new system to complete the PTP control system. Since the yaw axis is not disturbed by the gravity torque and can be stabilized by itself, the yaw axis in the model is obtained by using the open-loop identification method. On the pitch axis, the deflection away from the equilibrium point(the angle when tilt parallels to the horizontal plane) arising from the gravity torque requires external forces to maintain stability. Therefore, the pitch axis in the model is obtained by closed-loop identification. The experimental results show that the control system has the advantages of both flexibility and strong adaptability.

2. Motivation and Contribution

(i) The multiple identifications we use can identify the interference factors introduced by each new controller. In the next controller design, the model can be made closer to the real situation, and the influence of the interference amplified on the system will not be increased due to the increase of the controllers' number

(ii) The system identification method we use can reduce the index measurement work, and integrate the difficult-to-measure parameters links into the transfer function of the system by identification, which solves the problem that the model modeling is inaccurate.

(iii) Pitch and Yaw are treated as two independent controlled objects, and they are decoupled. The Pitch uses closed-loop identification to solve the interference of gravity on Pitch. While the Yaw uses open-loop identification to reduce the difficulty of system identification.

3. Overall structure of the control system

3.1. Pan-tilt platform

A two-axis PTP is a two-degree-of-freedom rotary platform that consists of a horizontally rotatable yaw axis and a vertical pitch axis. Two motors are used to drive the yaw axis and the pitch axis independently. Figure 1 shows the PTP system considered in the paper. The pitch motor is a RM6623 brushless DC motor, and the yaw motor is a DM9015 brushless DC motor. The basic parameters of the motor used in the design control system are listed in Table 1. By comparing the parameters of the PTT motor and the actual needs, we believe that this motor can meet the basic requirements of this PTP design. The DM9015 disc motor has a through hole in the center, where the slip ring could get through. In this way, we can make it as a 360º pan/tilt while providing electric power and signal to the pitch motor, which makes the PTP more flexible.

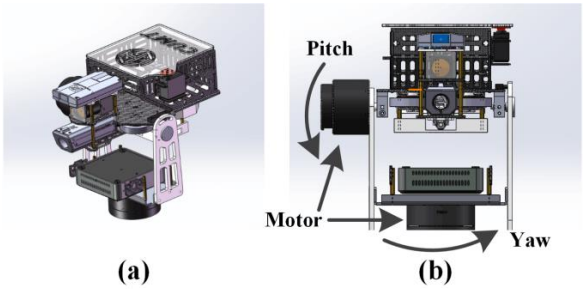

Figure 1. (a) PTP 3D figure and (b) illustration of the PTP.

Table 1. Motor parameters.

Item	RM6623	DM9015
Weight	605g	560g
Torque Constant	0.38N•m/A	0.53N•m/A
Speed Constant	25RPM/V	19.5RPM/V
Torque	2N•m	5.93N•m
Stall Current	5.3A	11.2A
Rated Rotational Speed	600RPM	390RPM

The through hole designed in the middle of the motor can accommodate a conductive sliding ring to realize 360° omnidirectional rotation of the yaw axis, which increases the flexibility of PTP significantly. We use the STM32F405 microcontroller unit as the computing unit.

3.2. Control System Structure

The control diagram for the PTP is shown in Figure 2, where $G(s)$ is the transfer function of a controller and θ denotes the angular displacement. Here, θ_{in} is the target value of the input angle, and θ_{out} is the output of the current angle value. The motor angular velocity ω_{gyro} is obtained as an angular velocity feedback by the gyroscope. The pan/tilt position $\theta_{encoder}$ is obtained by measuring the motor with a magnetic encoder, and the signal is normalized to the dimension of θ_{in} by unit conversion as an output. The two axes of the PTP are independently controlled, and each axis uses a double loop controller that contains a speed loop and a position loop. The output of the speed controller is sent to the current controller, which contains an integrated current loop. The angular velocity is measured by a gyroscope mounted on the PTP and fed back to the speed controller. The positional information is fed back by the magnetic encoder mounted on the motor.

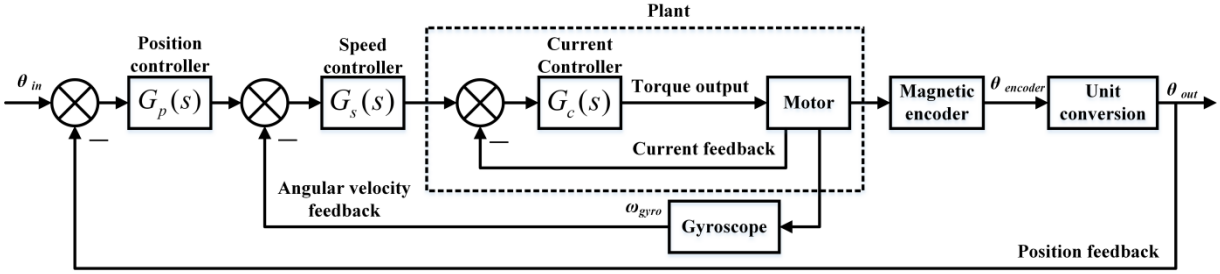

Figure 2. Continuous system control scheme. The control scheme includes a position controller $G_p(s)$ and a speed controller $G_s(s)$. The DC motor contains an integrated current controller $G_c(s)$.

In the actual applications, the angular velocity feedback from the gyroscope cannot be directly compared with the output of the position controller. Since the angular velocity of gyro feedback is not measured in degrees, unit conversion is required:

$$\omega = \omega_{gyro} \div 32.768 \tag{1}$$

where ω is the angular velocity in the angle system, ω_{gyro} is the angular velocity measured by the gyroscope, and 32.768 corresponds to 32.768 LSB/(°/s). The PTP controller is typically implemented with digital devices; thus, the continuous system shown in Figure 2 can be discretized with a sampling period of 0.001 seconds.

Since the current loop is integrated in the current controller, the current controller can be integrated with the motor. After the PTP is physically constructed, each axis is artificially set at 0 degrees, but the value of the motor encoder is not 0; thus, we have to subtract the initial value. Since the encoder feeds back an absolute position and the feedback value is within [0, 8191], we need to consider the situation of zero crossing. To couple the dimensions of θ_{in} and θ_{out}, we convert the absolute position feedback of the encoder into an incremental form $\theta_{encoder}$. Finally, the incremental form value of the encoder feedback is converted into the incremental form value of the output angle θ_{out} by unit conversion:

$$\theta_{out} = \theta_{encoder} \div 22.756 \tag{2}$$

where 22.756 corresponds to 22.756 LSB/degree. We also convert the input to incremental form θ_{in} to achieve unit negative feedback in the position closed loop. In the continuous system, the angular velocity can be used to calculate the angle by integration. Since the angle incremental form value can be fed back by the gyroscope, the unit of the gyroscope feedback is converted to degrees per second. The integral element should be transferred into $\frac{0.0305}{s}(\frac{1}{s} \div 32.768 = \frac{0.0305}{s})$.

The sample time equals 0.001 seconds, we can discretize the system with a zero-order holder. The integral element now changes to $\frac{3.052\times10^{-5}}{z-1}$. The actual PTP control system in the discrete form is shown in Figure 3. In Figure 3, $G_0(z)$ is the plant that we need to identify. The discrete controllers $G_s(z)$ and $G_p(z)$ are the ones that we are going to design. Here, the Φ_{speed} is a closed loop with a speed controller, and the Φ_{speed} linked with a integral section consists the Φ_{core}.

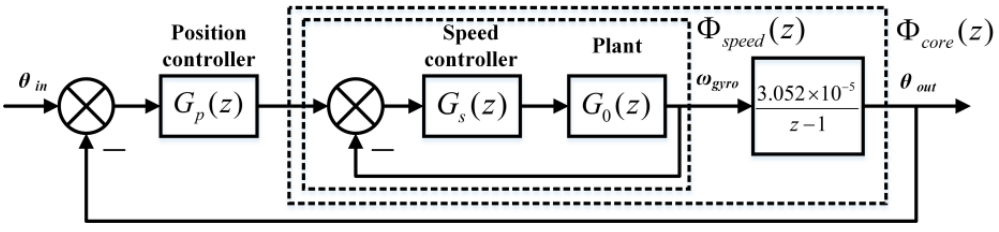

Figure 3. Discrete PTP control scheme containing the position and speed controller.

4. Modeling and design of the controllers on the yaw axis

4.1. Modeling

The horizontal rotation around the yaw axis is not affected by the gravity torque factor and can be

stabilized without external force. Therefore, the controller can be designed by using the open-loop system identification method. Input the yaw axis motor with a sinusoidal signal:

$$Signal = A\sin(2\pi ft) \tag{3}$$

where the amplitude A is set to 4000, which is determined according to the range of data defined in the current controller protocol. The frequency f is changed from 1 Hz to 500 Hz, and each frequency lasts for 20 cycles. Since the frequency bandwidth of the input signal is large, the amplitude variation of the PTP in the high-frequency portion is small; thus, we adjust the frequency f to increase almost exponentially. At the same time, it is necessary to guarantee that the input signal corresponding to each frequency starts from the zero phase.

Because the amplitude of the PTP changes little in the high-frequency part, the vibration frequency is faster, and the collected data may not reflect the true condition of the system due to the signal acquisition frequency and the lower resolution of the sensor. In this case, the frequency f can be appropriately reduced to improve the accuracy of the identification.

The gyroscope angular velocity feedback is acquired as a system output. By referencing other papers describing the mechanism model [1,5,14] and using the root locus analysis [15,16], we find that the number of the zeros of the PTP model is 0 and the number of poles is 2. The input and output are systematically identified by system identification. The discrete transfer function of the yaw axis is obtained, and the sample time is 0.001 seconds:

$$G_0^{Yaw}(z) = \frac{0.0006369}{1 - 1.898z^{-1} + 0.8986z^{-2}} \tag{4}$$

4.2. Speed Controller Design

The PID controller is simple, reliable, and easy to implement on MCU; thus, it is widely used in industrial fields. The controller of this paper needs to be implemented on MCU, and the system is required to be stable and reliable; therefore, the PID controller is adopted. Because the PTP fast response speed is required and the deviation is small on this basis, besides, gyroscope's feedback frequency is high, so that only the proportional element in the speed controller is required. Its transfer function reads

$$G_s^{Yaw}(z) = 14.3211 \tag{5}$$

4.3. Position Controller Design

Here, we introduce the speed loop controller $G_s^{Yaw}(z)$ into the control system. When a new section is added to the control model, the error increases between the idealized model and the real model. Inconsistency inevitably arises between the closed-loop transfer function $\Phi_{speed}^{Yaw}(z)$ and the real model due to various uncertain factors. In addition, model augmentations and an interference factor may be introduced to the entire system. Therefore, re-identification should be performed to identify a new model and design the position controller based on it.

To design the position controller, the measurements by the magnetic encoder are read and converted as the feedback of the system. In Figure 3, an integral element is introduced between ω_{gyro} and θ_{out}, namely, $\frac{3.052\times10^{-5}}{z-1}$, to increase the number of poles. The result indicates that the new model has 0 zeros and 3 poles. After the re-identification of the speed closed-loop together with the integral element, we obtain the discrete transfer function:

$$\Phi_{core}^{Yaw}(z) = \frac{8.48\times10^{-7}}{1 - 2.836z^{-1} + 2.701z^{-2} - 0.8646z^{-3}} \tag{6}$$

The position controller $G_p^{Yaw}(z)$ can be designed based on the transfer function $\Phi_{core}^{Yaw}(z)$, where we use the integral separation PI controller

$$G_p^{Yaw}(z) = \frac{1971 - 1935z^{-1}}{1 - z^{-1}} \tag{7}$$

The integral element works when the bias $|\theta_{in} - \theta_{out}| \le 2^{\circ}$, and the output of the integral element is limited to [-3000,3000].

4.4. System Performance Analysis

To analyze the performance of the designed control system, we input a sinusoidal signal similar to Equation (3). For comparison, we build a set of controllers by experience. With varying amplitude *A* and frequency f, we obtain the step response, bode diagram and tracking curves shown in Figure 4 and Figure 5. The reference signal shown in Figure 5 is the same as that in Equation (3).

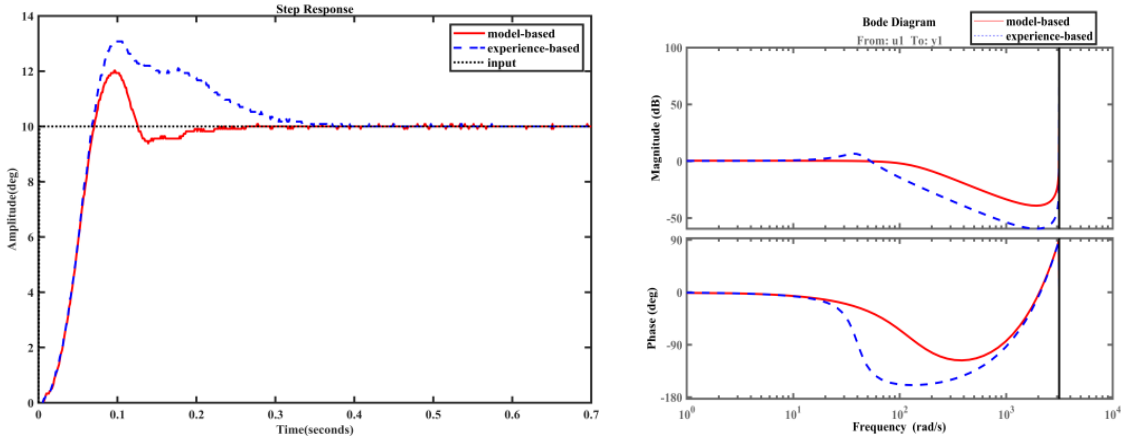

Figure 4. Step response and Bode diagram of the control system on the yaw axis.

Table 2. Performance comparison between the model-based and experience-based control system on the yaw axis.

Item	Model-based	Experience-based
Bandwidth	120rad/s	63 rad/s
Rise time	0.071s	0.068s
Settling time	0.181s	0.282s
Overshoot	20.2%	32.5%

As shown in Figure 4, the model-based controller can increase the bandwidth of the system substantially and reduce the settling time. The results indicate that the rise time is essentially unchanged, while the overshoot is decreased. Figure 5 shows that when the system is operating at low frequency, the performance of the model-based and the experience-based controllers is almost identical. In this stage, the input signal can be well matched. In Table 2, with increasing frequency, the lag time of model-based controller is slightly longer, the precision is slightly decreased, but the performance is clearly better than that of the experience-based controller. On the yaw axis, the method of this paper greatly reduces the settling time and overshoot, and improves the tracking performance. The yaw control system established by system identification is robust and fast in response and exhibits strong tracking performance.

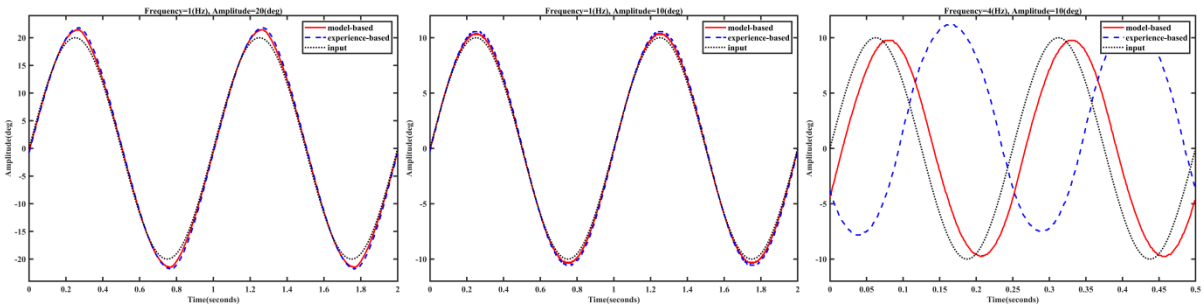

Figure 5. Tracking curve of the control system on the yaw axis.

5. Pitch axis Modeling and design of motion systems

5.1. Modeling

Due to the influence of gravity torque, the controller can maintain stability only by applying an external force. Therefore, the controller is designed using a closed-loop system identification. The unsimplified pitch control system in the discrete form is shown in Figure 6. Here, $H(z)$ is a nonlinear gravity compensation component, which could be calculated with the cross-angle between the PTP and the ground surface(θ_{out}) and the motor torque curve function. Through the motor torque curve function, we can know the relationship between the motor torque increment and the input increment.

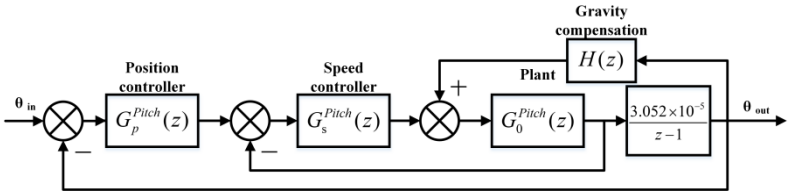

Figure 6. Discrete control structure on the pitch axis.

Since the pitch axis is affected by gravity torque, the speed loop should be compensated according to the current angle. The pitch axis rotating angle ranges from -30º to 30º, when it is 0º, the force of the gravity torque acting on the rotating shaft is $T_0 = mgr$, where *mg* is the gravity on the center of gravity of the pitch and *r* is the distance from the center of gravity to the axis of rotation. When the pitch rotation angle is 30º, the force of gravity torque acting on the rotating shaft $T_0 = mgr * \cos(30^\circ)$. Since *mg* and *r* are relatively small and the torque is barely changed under the rotation angle of the PTP, we do not adopt the gravity torque compensation element $H(z)$. Therefore, the pitch control structure we adopt is similar to the yaw control structure shown in Figure 3. Note that although the control system structure on the pitch axis is the same as that on the yaw axis, the identification procedures are completely different due to the gravity torque on the pitch axis.

We develop the speed closed-loop control system based on experience, that is, we design a suitable speed controller $G_s^{*Pitch}(z)$ and drive the PTP to a stable state. Here, we obtain $G_s^{*Pitch}(z) = 2$. Then, we develop the model of the speed closed-loop system by system identification. The input to the system is a sinusoidal signal with amplitude *A*=3000,

$$Signal = A\sin(2\pi ft) + B \tag{8}$$

where the frequency *f* also increases exponentially and *B* is the compensation value. Since the center of gravity of the PTP is not on the axis of rotation, the PTP slides in one direction under the influence of gravity torque. Because there are mechanical limits on the pitch axis, the feedback data are

invalidated when the PTP is out of range. When the tilt angle is too large, the compensation value forces the pitch axis deflection in the horizontal direction. When the tilt is close to the horizontal position, the compensation value *B* is reduced or canceled. In this paper, when the pitch angle exceeds 20°, *B* equals 500; when the pitch angle is less than -20°, *B* equals -300. The angular velocity feedback of the gyroscope is read as the output of the system. The input and output are systematically identified to obtain the discrete transfer function of the control system. The sample time is 0.001 seconds as well, and we obtain

$$\Phi_{speed}^{Pitch}(z)=\frac{0.009593}{1-1.885z^{-1}+0.8954z^{-2}} \tag{9}$$

Together with $\Phi_{speed}^{Pitch}(z)$ and $G_s^{*Pitch}(z)$, $G_0^{Pitch}(z)$ is calculated as

$$G_0^{Pitch}(z)=\frac{0.009593}{1.981-3.771z^{-1}+1.791z^{-2}} \tag{10}$$

5.2. Controller Design

Using the transfer function $G_0^{Pitch}(z)$, we design the speed controller $G_s^{Pitch}(z)$, that is,

$$G_s^{Pitch}(z)=1.7572 \tag{11}$$

Similarly, we first design a suitable position controller $G_p^{*Pitch}(z)=1000$ by experience, and we define the entire Figure 3 as $\Phi_{all}^{Pitch}(z)$. By using the input signal in Equation (3) with the amplitude *A*=20, we identify the discrete transfer function of the entire control system with 0 zeros and 3 poles and obtain

$$\Phi_{all}^{Pitch}(z)=\frac{0.01068}{1\text{-}0.7992z^{-1}+0.9946z^{-2}+0.8045z^{-3}} \tag{12}$$

From $\Phi_{all}^{Pitch}(z)$ and $G_p^{*Pitch}(z)$, we can calculate

$$\Phi_{core}^{Pitch}(z)=\frac{1.068\times10^{-5}}{1\text{-}0.7992z^{-1}+0.9946z^{-2}+0.8045z^{-3}} \tag{13}$$

Based on the re-identified transfer function $\Phi_{core}^{Pitch}(z)$, the position controller on the pitch axis is designed as a integral separation PI controller

$$G_p^{Pitch}(z)=\frac{1618\text{-}1523z^{-1}}{1\text{-}z^{-1}} \tag{14}$$

The integral element works when $\left|\theta_{in}-\theta_{out}\right|\le 3^{\circ}$, and the output of integral element is constrained to [-3000,3000].

5.3. System Performance Analysis

The step response and Bode diagram are shown in Figure 7. The model-based controller can greatly increase the bandwidth of the system, significantly reduce the settling time, and reduce overshoot. Since the pitch axis is subjected to considerable external interference, the model-based controller is very important for system performance improvement. When the system operates at low frequency, the performance of the model-based controller is similar to that of the experience-based controller, which is shown in Figure 8. As the frequency increases, the lag time of the model-based controller becomes slightly longer, the accuracy decreases slightly, but the performance of the experience-based controller decreases significantly, particularly in overshoot. The performance comparison is shown in Table 3. The pitch axis control system established by system identification is robust and fast in response and exhibits strong tracking performance.

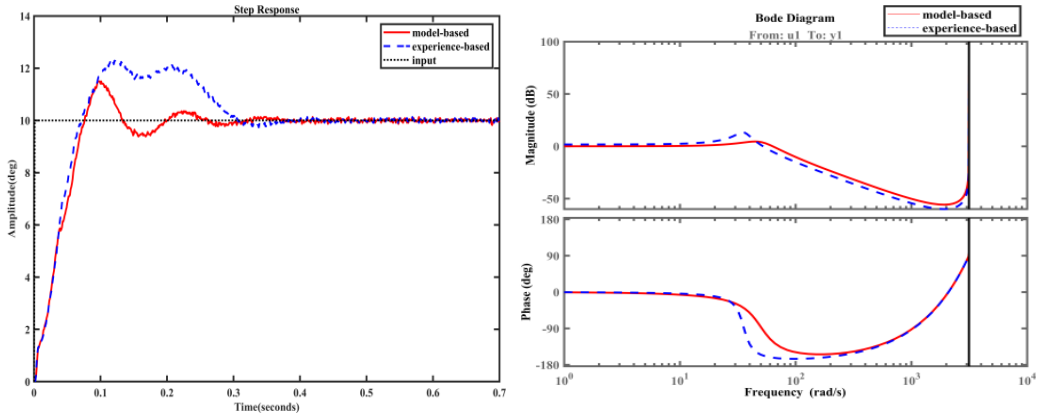

Figure 7. Step response and Bode diagram of the control system on the pitch axis.

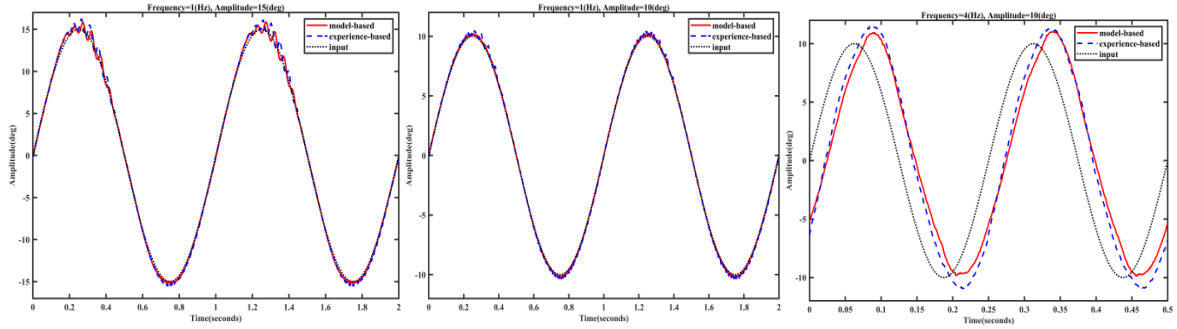

Figure 8. Tracking performance on the pitch control system.

Table 3. Performance comparison between the model-based and experience-based control system on the Pitch axis.

Item	Model-based	Experience-based
Bandwidth	70rad/s	57 rad/s
Rise time	0.075s	0.071s
Settling time	0.175s	0.283s
Overshoot	14.9%	23.7%

6. Conclusions

This paper proposes a simple and efficient method of system identification and controller design for a two-axis pan-tilt platform. The model established by system identification does not need to identify the parameters such as the resistance and response lag of the PTP, which is beneficial to the subsequent controller design. The entire control system is designed with an inside-out approach, ensuring that each element is optimized to meet the requirements so that the entire controller can provide suitable performance.

Acknowledgments

This work is supported in part by the Science and Technology Program of Xuzhou (Grant No. KC18069) and the Laboratory Open Funds of China University of Mining and Technology (Grant No. 20180217).

References

[1] I. S. Sarwar and A. M. Malik, Modeling, analysis and simulation of a Pan Tilt Platform based on linear and nonlinear systems, 2008 IEEE/ASME International Conference on Mechtronic and Embedded Systems and Applications, Beijing, pp. 147-152 (2008)
[2] G. Binkun, Research on Intelligent Control Algorithm for UAV Three-axis Self-stable Pan-tilt, Diss, JiMei University (2013)
[3] Z. Xin, Y. Fang, G. Zhang and H. Shen, Experiment platform for pan-tilt control of a small scale autonomous helicopter, Proceedings of the 29th Chinese Control Conference, Beijing, pp. 3544-3547 (2010)
[4] Naung, A. Schagin, H. L. Oo, K. Z. Ye and Z. M. Khaing, Implementation of data driven control system of DC motor by using system identification process, 2018 IEEE Conference of Russian Young Researchers in Electrical and Electronic Engineering (EIConRus), Moscow, pp. 1801-1804 (2018)
[5] I. S. Sarwar, J. Iqbal, and A. M. Malik, Modeling, analysis and motion control of a pan tilt platform based on linear and nonlinear systems, WSEAS Transactions on Systems and Control 4.8, pp. 389-398 (2009)
[6] H. Zhong-xu, Q. Xiao-hong, L. Min, Z. Zhi and Z. Chuan-xin, Mixed Boiler-turbine Coordinated Control System Mathematical Model Based on Mechanism Modelling and Parameter Identification, 2006 1ST IEEE Conference on Industrial Electronics and Applications, Singapore, pp. 1-5 (2006)
[7] Z. Song, Y. Lin, X. Mei and G. Jiang, A Novel Inertia Identification Method for Servo System Using Genetic Algorithm, 2016 International Conference on Smart Grid and Electrical Automation (ICSGEA), Zhangjiajie, pp. 22-25 (2016)
[8] R. Fung and W. Yang, System identification of an induction motor, 2017 International Conference on Applied System Innovation (ICASI), Sapporo, pp. 1068-1071 (2017)
[9] W. Tang, Z. Liu and Q. Wang, DC motor speed control based on system identification and PID auto tuning, 2017 36th Chinese Control Conference (CCC), Dalian, pp. 6420-6423 (2017)
[10] S. Xie, J. Luo, P. Xie, Z. Gong and H. Zou, Biomimetic Control of Pan-tilt-zoom Camera Mounted on an Autonomous Helicopter, 2007 International Conference on Mechatronics and Automation, Harbin, pp. 2003-2008 (2007)
[11] H. Chen, X. Zhao and M. Tan, A novel pan-tilt camera control approach for visual tracking, Proceeding of the 11th World Congress on Intelligent Control and Automation, Shenyang, pp. 2860-2865 (2014)
[12] M. A. Olivares-Méndez, P. Campoy, C. Martínez and I. Mondragón, A pan-tilt camera Fuzzy vision controller on an unmanned aerial vehicle, 2009 IEEE/RSJ International Conference on Intelligent Robots and Systems, St. Louis, MO, pp. 2879-2884 (2009)
[13] S. Sharp, A. Wicks, A. Ordys and G. Collier, Modelling of a pan and tilt servo system, Proceedings of 2012 UKACC International Conference on Control, Cardiff, pp. 546-550 (2012)
[14] Aihua Zhang, and Jianfei NI, Uniaxial turntable control system based on fuzzy self-adaptive PID, Journal of Heilongjiang University of Science & Technology (2015)
[15] W. R. Evans, Control System Synthesis by Root Locus Method, Transactions of the American Institute of Electrical Engineers, vol. 69, no. 1, pp. 66-69 (1950)
[16] N. S. Nise, Control systems engineering, Wiley student edition, Fourth edition, pp. 515-524 (2004)